ARTICLES
PUBLISHED ONLINE: 30 MARCH 2014 | DOI: 10.1038/NNANO.2014.44
nature nanotechnology

High thermal conductivity of chain-oriented amorphous polythiophene

Virendra Singh[1†], Thomas L. Bougher[1†], Annie Weathers[2], Ye Cai[3], Kedong Bi[2,4], Michael T. Pettes[2], Sally A. McMenamin[2], Wei Lv[1], Daniel P. Resler[5], Todd R. Gattuso[5], David H. Altman[5], Kenneth H. Sandhage[3], Li Shi[2], Asegun Henry[1,3] and Baratunde A. Cola[1,3]*

Polymers are usually considered thermal insulators, because the amorphous arrangement of the molecular chains reduces the mean free path of heat-conducting phonons. The most common method to increase thermal conductivity is to draw polymeric fibres, which increases chain alignment and crystallinity, but creates a material that currently has limited thermal applications. Here we show that pure polythiophene nanofibres can have a thermal conductivity up to ~4.4 W m^{-1} K^{-1} (more than 20 times higher than the bulk polymer value) while remaining amorphous. This enhancement results from significant molecular chain orientation along the fibre axis that is obtained during electropolymerization using nanoscale templates. Thermal conductivity data suggest that, unlike in drawn crystalline fibres, in our fibres the dominant phonon-scattering process at room temperature is still related to structural disorder. Using vertically aligned arrays of nanofibres, we demonstrate effective heat transfer at critical contacts in electronic devices operating under high-power conditions at 200 °C over numerous cycles.

Bulk polymers are commonly considered thermal insulators because of their low thermal conductivities, on the order of 0.2 W m^{-1} K^{-1} at room temperature. We find no reports of this value being enhanced beyond a factor of 2 (~0.4 W m^{-1} K^{-1}) without the aid of crystalline domains in the polymer[1]. The low thermal conductivity of these materials is caused by the random orientation of the molecular chains in amorphous regions[1,2], which reduces the mean free path of heat-conducting phonons. Although light weight, low cost, corrosion resistance and manufacturability are attractive characteristics of polymers, such materials are currently used for thermal applications only in the form of composites that contain thermally conductive fillers[2].

It is well understood that increasing the crystallinity and aligning the crystallites of a polymer (Fig. 1a) leads to increased thermal conductivity[1]. Recent reports demonstrate that metal-like thermal conductivity (>100 W m^{-1} K^{-1}) can be achieved in ultra-drawn highly crystalline polyethylene[3]. It has also been found that some high-modulus commercial fibres have a thermal conductivity of more than 10 W m^{-1} K^{-1}, and the thermal conductivity versus temperature decays as $1/T$ at room temperature[4], consistent with the anharmonic phonon–phonon scattering that is dominant in highly crystalline materials. The experimental demonstrations of polymers with high thermal conductivity complement the findings of a number of simulations suggesting that the thermal conductivities of individual chains of certain polymers can be extremely high[1,5]. Such high thermal conductivity has thus far only been achieved in individual fibres, which are unsuitable for practical applications due to processing limitations[2].

Increasing the degree of crystallinity in polymers typically results in a proportional increase in both the elastic modulus[6–8] and the thermal conductivity[7,9], although some recent work has shown that these relationships are not universal for polymers[10]. Previous studies to enhance the thermal conductivity of polymers have focused on semicrystalline polymers such as drawn polyethylene that degrade at temperatures as low as 125 °C (ref. 11). Chain orientation within the amorphous regions of polymers (Fig. 1b) is also understood to increase thermal conductivity[1,12], although it is unclear whether significant chain alignment can be achieved without creating some crystalline domains. The increase in thermal conductivity through chain orientation in non-crystalline regions can only be studied properly through examination of a purely amorphous structure, which has not been demonstrated previously.

Here we show that polythiophene nanofibres can achieve thermal conductivity more than 20 times greater than the bulk polymer through chain alignment in a purely amorphous material via template-assisted electropolymerization. Figure 1 depicts the difference in morphology between chain alignment in semicrystalline (previous studies[1,4,7]) versus purely amorphous (this work) polymers. We show that the thermal performance of vertically aligned arrays of the polythiophene nanofibre over device-size areas is stable at 200 °C, which makes this material well-suited for use in high-temperature applications such as in power electronics in electric vehicles, waste heat recovery, and heat exchangers.

Fabrication and structure of polythiophene nanofibres

To fabricate polythiophene nanofibres with oriented chains, we electropolymerized vertically aligned arrays of polythiophene nanofibres (Fig. 1c) inside the aligned nanopore channels of anodic alumina templates. We measured the thermal conductivity of isolated solid fibres to study transport physics and of tubes in arrays

[1]George W. Woodruff School of Mechanical Engineering, Georgia Institute of Technology, 801 Ferst Drive, Atlanta, Georgia 30332, USA, [2]Department of Mechanical Engineering, The University of Texas at Austin, 204 East Dean Keeton Street, Austin, Texas 78712, USA, [3]School of Materials Science and Engineering, Georgia Institute of Technology, 771 Ferst Drive, J. Erskine Love Building, Atlanta, Georgia 30332, USA, [4]School of Mechanical Engineering, Southeast University, Nanjing, 211189, China, [5]Raytheon Company, Sudbury, Massachusetts 01776, USA. †These authors contributed equally to this work. *e-mail: cola@gatech.edu

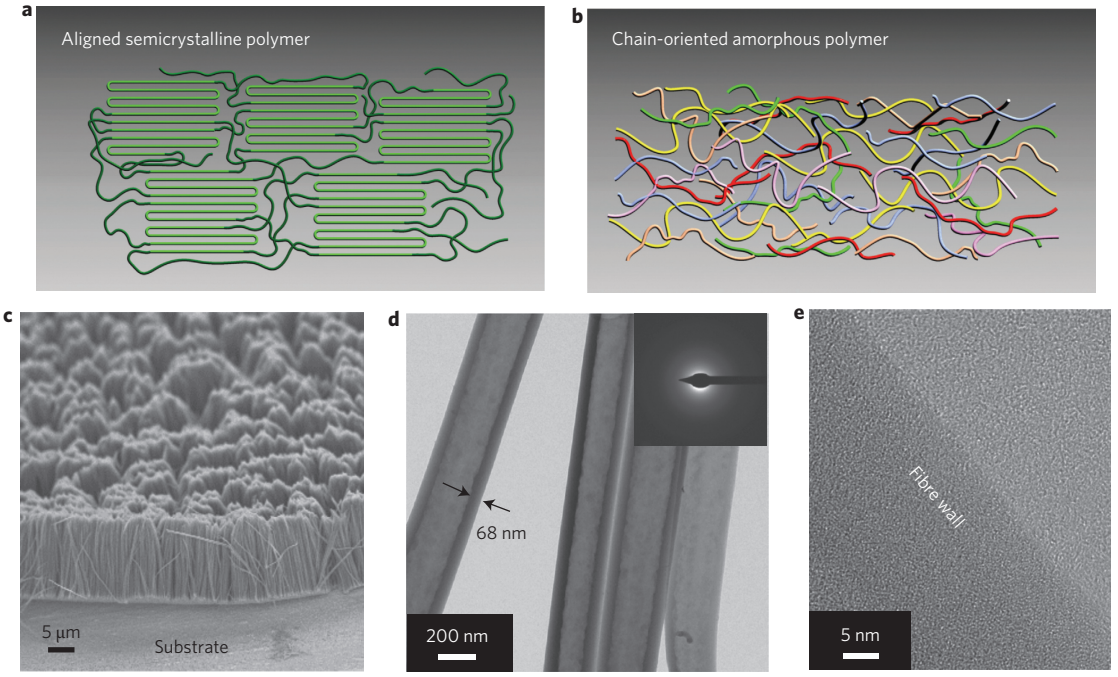

Figure 1 | Microstructure of polythiophene nanofibres. a, Chain orientation morphology in drawn semicrystalline polymer. The folded chains are crystallites or crystalline domains surrounded by amorphous regions. **b**, Chain orientation morphology in amorphous polymer: chain orientation without folded crystalline domains. The direction of heat transfer is horizontal in **a** and **b**. **c**, Scanning electron microscopy image of vertical polythiophene nanofibre arrays on a metal substrate. The arrays contained either solid fibres or mostly tubes depending primarily on pore diameter. Template pore channels of varying diameter (200, 100, 55 and 18 nm) control the fibre diameter, although template irregularities caused fluctuations about these nominal diameters (for example, the ranges of polythiophene nanofibre diameters from 200 nm and 100 nm templates were 145–300 nm and 70–120 nm, respectively). The smaller-diameter fibres (18 and 55 nm templates) did not remain vertically aligned after removing the template due to their reduced stiffness, making them more difficult to apply as heat transfer materials. **d**, TEM image of a polythiophene nanofibre from a 200 nm template. Inset: Selected-area electron diffraction analysis consistent with amorphous material. **e**, High-resolution TEM image of a polythiophene nanotube wall, showing amorphous material.

for large-area application as interface materials. An established procedure[13,14] was modified to attach the templates to metal substrates with areas as large as 12 cm^2 (Supplementary Fig. 2). The lengths of the nanofibres were controlled by the total charge passing through the electrochemical cell during polymerization (Supplementary Figs 3, 4) and varied from several micrometres up to tens of micrometres (Supplementary Table 1). Transmission electron microscopy (TEM) of polythiophene nanofibres from 200 nm templates revealed tubular structures with wall thicknesses ranging from 40 to 80 nm (Fig. 1d). (A few of the ~200-nm-diameter polythiophene nanofibres were solid fibres, and these were used for thermal conductivity measurements on single fibres in this diameter range.) The polythiophene nanofibres of smaller diameter were solid fibres (Supplementary Table 2). Such tube formation was consistent with the signature of two-dimensional growth observed in chronoamperograms (Supplementary Fig. 3) and the tendency of polymer chains to preferentially nucleate on pore walls, as mediated by the solvophobic effect[15]. The high surface energy of alumina may also facilitate interaction between the polymer chains and the pore walls, and promote chain expansion along the growth axis[16] and possibly prevent chains from folding into crystallites. Preferential chain orientation generally results from significant crystallinity in polymers (Fig. 1a)[7,9,17]. However, the polythiophene nanofibres of the present work, with diameters ranging from 18 to 300 nm, were found to be amorphous when analysed using electron diffraction (inset of Fig. 1d and Supplementary Fig. 5) and high-resolution TEM (Fig. 1e), at different locations along the fibre lengths. The amorphous nature of the fibres was also confirmed by X-ray diffraction (Supplementary Fig. 6). A sharp and strong band at ~1,455 cm^{-1} in the Raman spectra (Supplementary Fig. 7) indicates neutral conjugated segments[18] in the nanofibres.

To confirm and quantify molecular chain orientation in the polythiophene nanofibres, we used polarized infrared absorption spectroscopy[15]. Higher absorbance was observed with parallel polarization, indicating structural anisotropy within the material (Supplementary Fig. 9). The vibration band at 1,222 cm^{-1}, corresponding to C_α–C_α inter-ring stretching along the polythiophene backbone[19], was used to estimate the dichroic ratio and orientation function. A dichroic ratio greater than 1 indicates preferential molecular chain alignment and can be used to estimate the percentage of chains aligned parallel to the fibre axis[16]. Representative samples of the ~200-nm-diameter tube arrays had a dichroic ratio of 2.0 ± 0.2 and $25 \pm 4\%$ preferential orientation (for details see Supplementary Equations S1–S3). The dichroic ratio and degree of orientation increased to 3.2 ± 0.3 and $42 \pm 3\%$, respectively, for representative samples of the ~100-nm-diameter fibre arrays. These data clearly indicate a distinct degree of chain orientation along the amorphous polythiophene nanofibre axis, as illustrated in Fig. 1b, which increased significantly as the fibre diameter decreased.

Thermal conductivity of individual fibres

The thermal conductivity of individual nanofibres was measured using a suspended microbridge[20] (Fig. 2a,b). The measured thermal conductivity of the several nanofibre samples increases with decreasing diameter (Fig. 2a), a trend that agrees with the chain orientation measurements. The thermal conductivity of solid nanofibres with diameters of 204 ± 10 and 71 ± 3 nm increased monotonically from 100 to 350 K (Fig. 2b), which was consistent for all fibres measured. Although the thermal conductivities of certain amorphous materials reach approximately constant values by 300 K (ref. 21), those of carbon black[22], SiO_2 (ref. 21), some

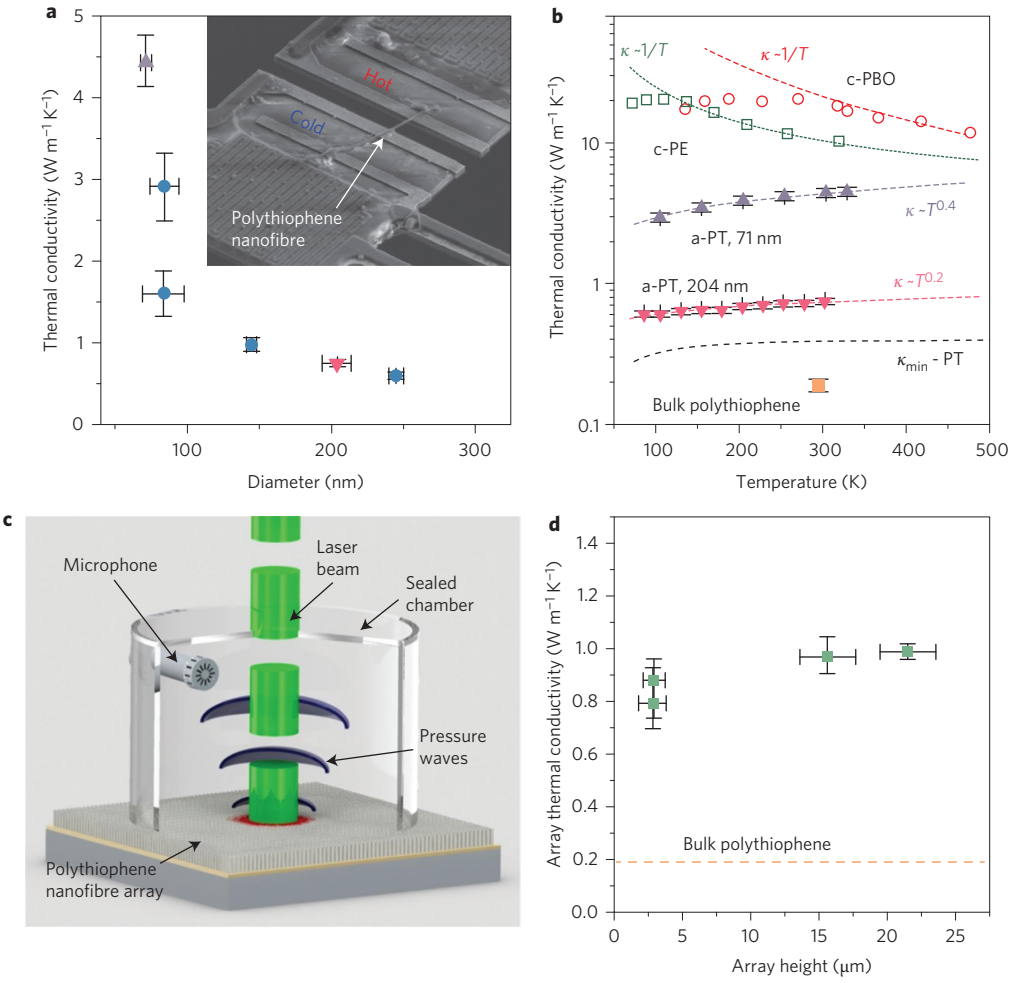

Figure 2 | Thermal conductivity measurements of single fibres and vertically aligned arrays. a, Single-fibre thermal conductivity at room temperature as a function of fibre diameter. Inset: Scanning electron microscopy image of a polythiophene nanofibre on a suspended microbridge for thermal conductivity measurement. **b**, Representative single-fibre thermal conductivity measurements on the microbridge as a function of temperature (the horizontal error bars are approximately the width of the data marker in all cases). The error bars in **a** and **b** are explained in the section 'Microbridge technique' in the Supplementary Information. Data of amorphous polythiophene (a-PT) fibres with different diameters (specified in the plot) are from this work. Crystalline polyethylene (c-PE) and crystalline polybenzobisoxazole (c-PBO) data are measurements reported in ref. 4. Black dashed line represents the predicted minimum thermal conductivity, κ_{min},[21] for polythiophene. **c**, Photoacoustic cell used to measure array thermal conductivity. **d**, Effective polythiophene nanotube (~200 nm diameter) array thermal conductivity as a function of height for vertically aligned arrays (60% fill fraction assuming solid fibres). The values for bulk polythiophene in **b** and **d** were obtained from photoacoustic measurements on electrodeposited films. Explanation of the error bars is given in the section 'Photoacoustic technique' in the Supplementary Information.

hydrogenated silicon films[23], as well as some polymers (polyethylmethacrylate and polyvinylchloride)[1] are still increasing at this temperature. The fibres in the present work exhibit a distinct trend of temperature-dependent thermal conductivity when compared with two commercial high-modulus fibres—polyethylene and polybenzobisoxazole (PBO) (Fig. 2b)—as measured with time-domain thermoreflectance[4]. Both commercial fibres are drawn with a high degree of crystallinity and exhibit a $1/T$ decay in thermal conductivity at room temperature and above[4]. In contrast, the thermal conductivity of the polythiophene nanofibre increases modestly at 300 K ($\kappa \approx T^{0.4}$ for $d = 71$ nm and $\kappa \approx T^{0.2}$ for $d = 245$ nm). The dominant phonon-scattering mechanism in the crystalline fibres at room temperature is anharmonic phonon–phonon (umklapp) scattering, but the nanofibres in the present work appear still to be dominated by interchain scattering due to disorder, despite some degree of chain orientation. It is likely that the polythiophene nanofibre has a strong increase in short-range ordering, and long-range order remains absent.

In highly disordered amorphous solids, the concept of a phonon (that is, propagating lattice vibration with a defined wavevector) loses meaning and is replaced by vibrational states called diffusons that are neither fully localized nor propagating[24,25], which is the basis of the minimum thermal conductivity theory[21]. Recent work has shown that even disordered solids can have phonon-like modes that propagate hundreds of nanometres[23,26], which is in conflict with this concept. Despite some shortcomings, the minimum conductivity theory can still provide reasonable agreement with some polymers[4] and is plotted in Fig. 2b. The predicted minimum thermal conductivity is a factor of ~2 higher than the thermal conductivity of bulk polythiophene and plateaus at ~300 K. This prediction is based upon the bulk speed of sound, but if the speed of sound in the polythiophene nanofibre was significantly increased by the chain orientation, as one might expect[27], the thermal conductivity would still be increasing at 300 K, as we have observed in the polythiophene nanofibre. The room-temperature thermal conductivity of the 245 ± 5, 204 ± 10, 145 ± 2, 84 ± 14,

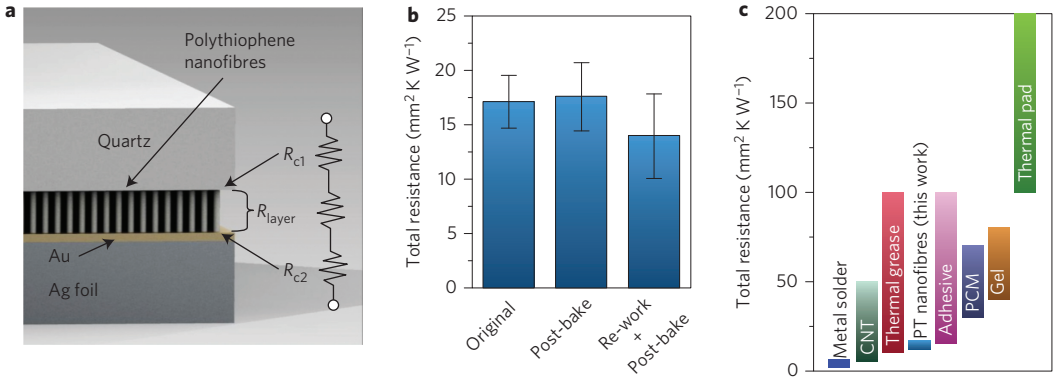

Figure 3 | Application of vertically aligned polythiophene nanofibres as a TIM. a, TIM illustration with component thermal resistances. The total thermal resistance of a TIM is a function of the layer thermal conductivity κ, layer thickness L and contact resistance R_{c1}, R_{c2} on each side of the material, and is given by $R_{total} = R_{c1} + R_{layer} + R_{c2}$ where $R_{layer} = L/\kappa$. **b**, Total thermal resistance measurements of polythiophene-nanotube TIMs with the photoacoustic technique. Post-bake data were obtained after the sample was heated in air for 100 h at 200 °C. Re-work + post-bake data were obtained after the same sample was wetted, removed from the quartz, then rewetted and dried on the quartz. Error bars represent one standard deviation of four to six measurements on each TIM. **c**, Comparison of total resistance values associated with a number of commercial TIM technologies. Values for carbon nanotube tubes (CNT) were obtained from refs 33 and 34, for thermal grease from refs 11 and 30, and for all others from ref. 30.

84 ± 12 and 71 ± 3 nm fibres were found to be 0.6 ± 0.1, 0.8 ± 0.1, 1.0 ± 0.1, 1.6 ± 0.3, 2.9 ± 0.4 and 4.4 ± 0.3 W m^{-1} K^{-1}, respectively (Fig. 2a), the last of which is 23 times higher than for bulk polythiophene (0.19 ± 0.02 W m^{-1} K^{-1}, as measured on a film using the photoacoustic technique). The differences in thermal conductivity of the three fibres with diameters between 71 and 84 nm are an indication of fibre-to-fibre variability in chain alignment, and an average thermal conductivity of 3.0 W m^{-1} K^{-1} should be used when comparing the fibre diameters to consider size effects. It is worth noting that these values are the apparent thermal conductivity of individual nanofibres and are lower than the intrinsic diffusive thermal conductivity because of the presence of contact thermal resistance in the two-probe thermal measurement. The contact resistance could be appreciable for the fibres of diameter 71 and 145 nm (Supplementary Fig. 11), but it is small for the other fibres.

Molecular dynamics simulations

We calculated the thermal conductivity of a single polythiophene chain using molecular dynamics (MD) simulations to estimate the upper limit of thermal conductivity. We used equilibrium MD simulations to calculate the thermal conductivity of individual polythiophene chains employing periodic boundary conditions at the chain ends. The simulations were run for 3 ns, and five independent simulations were run for better averaging, resulting in an average thermal conductivity of 43.3 W m^{-1} K^{-1} for chains ~40 unit cells in length (~32 nm). This result suggests that our material is not currently limited by the individual chain conductance and also that phonon transport along chains in the direction of heat transfer is probably responsible for the observed increase in thermal conductivity. Estimation of the dominant phonon mean free paths in the polythiophene nanofibre would provide additional insight, but this information was difficult to extract from our experimental data and requires further study because a significant spectrum of mean free paths could contribute to thermal conductivity at room temperature, even for amorphous materials[26].

Nanofibre arrays as thermal interface materials

Large-area arrays of nanotubes with controlled heights are required to create a usable heat transfer material. Hence, the effective thermal conductivities of films of vertically aligned polythiophene nanofibres (~200-nm-diameter tubes) were measured using a photoacoustic technique[28] (Fig. 2c). Films with nanotube heights of 2–20 μm exhibited thermal conductivities (Fig. 2d) ranging from 0.8 to 1.0 W m^{-1} K^{-1} with little dependence on nanotube height. The estimated thermal conductivity of individual fibres within these films was 1.4 ± 0.3 W m^{-1} K^{-1} (Supplementary Fig. 19) assuming solid fibres with a fill fraction of 60% (estimated from the manufacturer's template pore density and diameter specifications). Further correction for the void space within the tubes (based on a diameter of 200 nm and a wall thickness of 40 nm from TEM images) yielded an estimated individual tube thermal conductivity of 2.2 ± 0.6 W m^{-1} K^{-1} with an overall fill fraction of ~38%. Because accurate measurement of tubes was not possible with the suspended microbridge, the single-fibre conductivities extracted from photoacoustic measurements are intended to provide an estimate for comparing tubes and solid fibres of similar diameters. The single-tube conductivity from photoacoustic measurements implies that tubes have higher thermal conductivity than solid fibres. Unfortunately, this trend could not be confirmed with chain alignment measurements using polarized infrared absorption spectroscopy as we were unable to grow arrays with mostly solid fibres in the 200-nm-diameter templates.

To demonstrate the potential usefulness of this material in an electronic device cooling application, thermal interface materials (TIMs) (Fig. 3a) were created directly on metal substrates using vertically aligned arrays of polythiophene nanofibres (Fig. 1c and Supplementary Fig. 2). The thermal resistances of three polythiophene nanofibre TIMs (with ~200-nm-diameter, 2- to 3-μm-tall tubes), measured using the photoacoustic technique, were 12.8 ± 1.3, 14.4 ± 3.3 and 17.1 ± 2.5 mm^2 K W^{-1}, respectively. The TIM was remarkably robust; that is, after thermal treatment for 100 h at 200 °C, detachment, and then reattachment, no appreciable increase in thermal resistance was detected (3% increase after baking, 18% decrease after reattachment) (Fig. 3b). The conjugated and aromatic structure of polythiophene offers good thermal stability and a high melting temperature due to strong alternating double bonds along its rigid backbone[29], and the decrease in resistance after reattachment probably resulted from small changes in the morphology of the tips that improved surface contact. The TIM resistances compared favourably with a number of commercial TIMs (Fig. 3c) and were significantly lower than the resistances of commercial TIMs (40–80 mm^{2}K W^{-1}) considered attractive for automotive applications at elevated temperatures[30]. To our knowledge, this is the only reported value for a pure polymer TIM, as the naturally

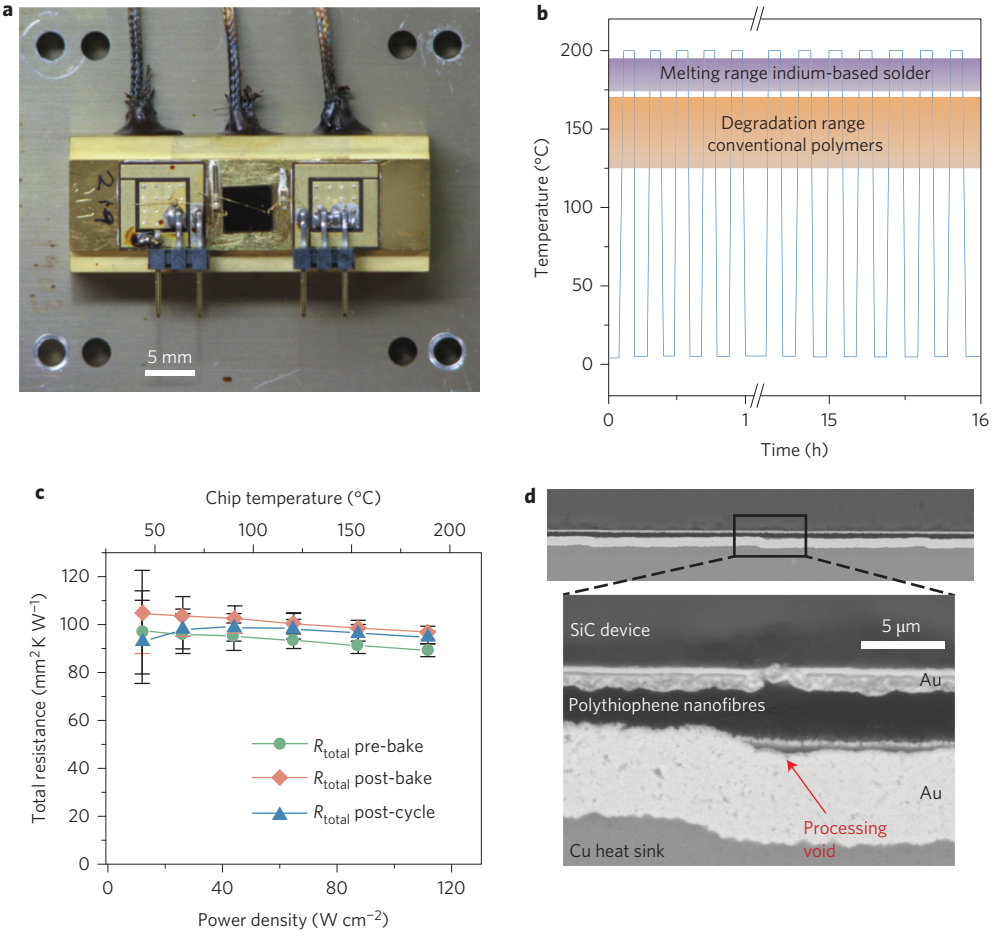

Figure 4 | Device demonstration of polythiophene-nanofibre TIM at high temperature. a, Polythiophene nanofibre array grown on a Cu heatsink and dried in contact with a SiC RF device simulator. **b**, Device operated while cycling in air between 5 °C and 200 °C for 16 h (80 cycles with 5 min dwell times at each temperature). **c**, Total thermal resistance R_{total} of the polythiophene nanofibre TIM measured as a function of power density before baking at 130 °C for 308 h (pre-bake), after baking (post-bake) and after thermal cycling (post-cycle) (as in **b**). Explanation of the error bars is given in the section 'Device testing' in the Supplementary Information. **d**, Cross-sectional scanning electron microscopy image of the device after testing. The magnified image reveals a void in the Cu heatsink that prevented the polythiophene nanofibre TIM from making good thermal contact.

low thermal conductivity of bulk polymers previously rendered this concept impractical.

As a further demonstration of the applicability of this material in devices, a polythiophene nanofibre TIM was integrated into a high-power silicon carbide radiofrequency (RF) device simulator (Fig. 4a), held at 130 °C for 308 h, and then thermally cycled in air between 5 and 200 °C a total of 80 times over 16 h (Fig. 4b). The total polythiophene nanofibre TIM resistance as a function of power density did not change noticeably after this aggressive thermal treatment and cycling (Fig. 4c), which was particularly noteworthy given the large mismatch in the thermal expansion coefficients of SiC and Cu (the difference is 1.2×10^{-5} K^{-1}) and the thin bond line (2–3 µm). To compare, the resistance of a common Ag-filled epoxy increased by 354% in only 36 cycles in the same test. It is important to note that the total resistance of the polythiophene nanofibre TIM decreased modestly as the temperature was increased up to 460 K. Given that the contact resistance is unlikely to change significantly with temperature, this implies that the thermal conductivity of polythiophene nanofibre continues to increase slowly at temperatures well above 300 K. The total resistance in the device was significantly higher (85–105 mm^2 K W^{-1} ± 10%) than in laboratory-scale tests, due to processing voids at the interface where the template was bonded to the Cu block (Fig. 4d). The high-temperature design target is 125 °C for military electronics and 140 °C for automotive applications[13], so the observed thermal stability of the polythiophene nanofibre TIM up to 200 °C makes it well suited to elevated-temperature applications where many other TIMs are unable to operate reliably[30]. At present, however, the polythiophene nanofibre TIMs are too thin and difficult to process for applications with significant surface roughness. They also provide less adhesive strength than typical solders and epoxies, so reinforcement could be required for their use in some applications.

Conclusions

We report the syntheses of amorphous polythiophene nanofibres with room-temperature thermal conductivities as high as 4.4 ± 0.3 W m^{-1} K^{-1}, which, to the best of our knowledge, is the highest value reported so far for an amorphous polymer and is among the highest lattice thermal conductivities reported for amorphous materials[22,31–34]. The polythiophene nanofibres, fabricated with a template-assisted electrochemical method, were found to have a degree of chain orientation along the fibre axis, and both the degree of chain orientation and thermal conductivity were observed to increase as the fibre diameter decreased. The enhanced polythiophene nanofibre thermal conductivity originates from the relatively high thermal conductivity of single oriented polythiophene chains, which is attenuated by phonon scattering from an

overall disordered structure. Our study provides an alternative means of obtaining polymers of high thermal conductivity via an increase in chain alignment without crystallization, using a fabrication process that is readily amenable for mass production. We demonstrated the significance of such thermal conductivity enhancement by fabricating (1) a polythiophene nanofibre interface material with a total thermal resistance as low as 12.8 ± 1.3 mm^{2}K W^{-1} and (2) a packaged electronic device exhibiting excellent stability of thermal resistance upon operation up to 115 W cm^{-2} at 200 °C over numerous cycles. This work demonstrates that a chain-oriented amorphous polymer can exhibit appreciably enhanced thermal conductivity compared with bulk polymers and reveals the potential of such amorphous polymer nanofibres as heat transfer materials for practical applications.

Methods

Nanofibre fabrication. Polythiophene nanofibres were synthesized electrochemically using a three-electrode one-compartment cell (Supplementary Fig. 1) with an electrolyte of thiophene in redistilled boron fluoride-ethyl ether. All solutions were deoxygenated with high-purity argon, and a slight overpressure of argon was maintained during fibre growth. A modified working configuration, described in the Supplementary Section 'Polythiophene nanofibre fabrication and isolation', was used to grow polythiophene nanofibres on metal surfaces. Details of the growth conditions for specific samples are provided in the Supplementary Table S1. To liberate the vertically aligned polythiophene nanofibre array, we treated the template with potassium hydroxide. The array was then neutralized with dilute hydrochloric acid and washed extensively with deionized water before further characterization.

Structural characterization. X-ray diffraction data were obtained with a PANanalytical diffractometer using Cu Kα radiation. Polythiophene nanofibre dispersions for microscopy were made by collecting the fibres using a centrifuge. TEM images and electron diffraction were collected on a Jeol 4000EX microscope. Polarized infrared absorption spectroscopy was used to study the degree of chain orientation in the nanofibres (Supplementary Figs 8, 10). Absorption data at two different polarizations were collected using a polarized infrared absorption spectroscopy microscope (FTS7000-UMA600) with a Perkin-Elmer wire grid polarizer. Additional details of these measurements are provided in the Supplementary Section 'Polarized infrared spectroscopy measurements'.

Thermal conductivity measurements of individual fibres. The suspended microbridge measurement device consisted of two adjacent SiN_x membranes, each patterned with a serpentine platinum resistance thermometer (PRT) and two electrodes and supported by six long, thin beams. A single polythiophene nanofibre was placed across the gap between the two membranes (Supplementary Fig. 12). Measurements were carried out in an evacuated cryostat with pressure on the order of 1×10^{-6} torr. A d.c. current supplied to one PRT raised its temperature by ΔT_h, and heat conduction through the sample caused a temperature rise in the adjacent sensing membrane of ΔT_s. The temperature rise in the heating and sensing membranes was measured from the temperature coefficient of resistance of the PRTs, and the thermal conductance of the nanofibre was determined from the total Joule heating and temperature difference between the heating and sensing membranes. Because of the low thermal conductance of some of the nanofibre samples, it was necessary to account for the background heat transfer between the two PRTs via residual gas molecules and radiation. To eliminate the background conductance, the temperature rise on the sensing membrane was measured relative to the temperature rise on the sensing membrane of a blank device with no nanostructure. The measured thermal resistance of the sample was expected to contain a contribution from the contact resistance between the nanofibre and the SiN_x membranes. The reported thermal conductivities and uncertainties do not include the effect of contact resistance because its magnitude is difficult to estimate. Additional details of microbridge measurements are provided in the Supplementary Section 'Microbridge technique'.

Thermal conductivity and interface resistance measurements of nanofibre arrays. The photoacoustic technique makes use of a modulated laser beam to periodically heat a sample in a closed volume where the thermal response of the sample is converted into pressure waves that are detected by a microphone and recorded using a lock-in amplifier (Supplementary Fig. 13). This technique was used to measure the total thermal resistance of polythiophene nanofibre TIMs and the thermal conductivity of polythiophene nanofibre arrays. Polythiophene nanofibre TIMs were measured by depositing a ~100 nm Ti layer on top of Ag foil to absorb the laser energy (Supplementary Fig. 14). Polythiophene nanofibre arrays were measured by absorbing the laser energy directly into the arrays. The thermal conductivity was determined from bare arrays for higher measurement sensitivity (Supplementary Figs 16, 17). The phase shift as a function of frequency was compared to a one-dimensional heat transfer model to extract thermal properties (Supplementary Figs 15, 18). Additional details about the photoacoustic measurements are provided in the Supplementary Section 'Photoacoustic technique'.

Thermal interface material attachment. The tips of the polythiophene nanofibre arrays were placed in contact with an opposing substrate in the wet state and allowed to dry under a fixed load (~200 kPa for 8–10 h under atmospheric conditions). Wetting the arrays with water, alcohol or FC-72 produced similar results. Based on adhesion testing (Supplementary Fig. 20), it appears that the tips adhere strongly to certain surfaces, such as quartz, through van der Waals interactions. The arrays were detached by simply rewetting the interface, and reattached by drying them in contact with the substrate again.

Simulated RF device testing. Thermal measurements were performed using a custom SiC Pt resistor-thermometer chip affixed to a Cu block heat-sunk to a temperature-controlled stage. Temperature data from a type-T thermocouple inserted into the Cu block were used to establish the relationship between temperature and resistance, which was essentially linear. Thermal resistance testing was then performed by varying the power dissipation of the resistor while performing a four-wire resistance measurement and measuring the block temperature. Thermal resistance was computed as the temperature difference between the resistor and thermocouple, divided by the power input to the resistor. Thermal interface resistance was obtained through numerical modelling of the configuration in ANSYS TAS v11.0. Thermal cycling was performed by applying and removing ~100 W of heat to the Pt resistor in 300 s intervals for 80 cycles, or until the sensed resistor temperature reached a cut-out limit of 250 °C.

Received 17 October 2013; accepted 11 February 2014; published online 30 March 2014; corrected after print 17 June 2014

References

1. Choy, C. L. Thermal conductivity of polymers. *Polymer* **18,** 984–1004 (1977).
2. Henry, A. Thermal transport in polymers. *Ann. Rev. Heat Transfer* http://dx.doi.org/10.1615/AnnualRevHeatTransfer.2013006949 (2013).
3. Han, Z. D. & Fina, A. Thermal conductivity of carbon nanotubes and their polymer nanocomposites: a review. *Prog. Polym. Sci.* **36,** 914–944 (2011).
4. Wang, X., Ho, V., Segalman, R. A. & Cahill, D. G. Thermal conductivity of high-modulus polymer fibers. *Macromolecules* **46,** 4937–4943 (2013).
5. Liu, J. & Yang, R. Length-dependent thermal conductivity of single extended polymer chains. *Phys. Rev. B* **86,** 104307 (2012).
6. Arkadii, A., Michael, B., Oleg, G. & Eyal, Z. Effect of supramolecular structure on polymer nanofibre elasticity. *Nature Nanotech.* **2,** 59–62 (2007).
7. Choy, C. L., Wong, Y. W., Yang, G. W. & Kanamoto, T. Elastic modulus and thermal conductivity of ultradrawn polyethylene. *J. Polym. Sci.* **37,** 3359–3367 (1999).
8. Lim, C., Tan, E. & Ng, S. Effects of crystalline morphology on the tensile properties of electrospun polymer nanofibers. *Appl. Phys. Lett.* **92,** 141908 (2008).
9. Choy, C. L., Chen, F. C. & Luk, W. H. Thermal conductivity of oriented crystalline polymers. *J. Polym. Sci.* **18,** 1187–1207 (1980).
10. Papkov, D. *et al.* Simultaneously strong and tough ultrafine continuous nanofibers. *ACS Nano* **7,** 3324–3331 (2013).
11. Prasher, R. Thermal interface materials: historical perspective, status, and future directions. *Proc. IEEE* **94,** 1571–1586 (2006).
12. Kurabayashi, K., Asheghi, M., Touzelbaev, M. & Goodson, K. E. Measurement of the thermal conductivity anisotropy in polyimide films. *J. Microelectromech. Syst.* **8,** 180–191 (1999).
13. Lu, G. *et al.* Drying enhanced adhesion of polythiophene nanotubule arrays on smooth surfaces. *ACS Nano* **2,** 2342–2348 (2008).
14. Xiao, R., Cho, S. I., Liu, R. & Lee, S. B. Controlled electrochemical synthesis of conductive polymer nanotube structures. *J. Am. Chem. Soc.* **129,** 4483–4489 (2007).
15. Martin, C. R. Nanomaterials: a membrane-based synthetic approach. *Science* **266,** 1961–1966 (1994).
16. Cannon, J. P., Bearden, S. D. & Gold, S. A. Effect of wetting solvent on poly (3-hexylthiophene)(P3HT) nanotubles fabricated via template wetting. *Synth. Met.* **160,** 2623–2627 (2010).
17. Shen, S., Henry, A., Tong, J., Zheng, R. & Chen, G. Polyethylene nanofibres with very high thermal conductivities. *Nature Nanotech.* **5,** 251–255 (2010).
18. Bazzaoui, E. A. *et al.* SERS spectra of polythiophene in doped and undoped states. *J. Phys. Chem.* **99,** 6628–6634 (1995).
19. Louarn, G., Buisson, J. P., Lefrant, S. & Fichou, D. Vibrational studies of a series of alpha-oligothiophenes as model systems of polythiophene. *J. Phys. Chem.* **99,** 11399–11404 (1995).
20. Shi, L. *et al.* Measuring thermal and thermoelectric properties of one-dimensional nanostructures using a microfabricated device. *J. Heat Transfer* **125,** 881–888 (2003).
21. Cahill, D. G., Watson, S. K. & Pohl, R. O. Lower limit to the thermal conductivity of disordered crystals. *Phys. Rev. B* **46,** 6131–6140 (1992).

22. Bullen, A. J., O'Hara, K. E., Cahill, D. G., Monteiro, O. & von Keudell, A. Thermal conductivity of amorphous carbon thin films. *J. Appl. Phys.* **88,** 6317–6320 (2000).
23. Liu, X. *et al.* High thermal conductivity of a hydrogenated amorphous silicon film. *Phys. Rev. Lett.* **102,** 035901 (2009).
24. Allen, P. B., Feldman, J. L., Fabian, J. & Wooten, F. Diffusons, locons and propagons: character of atomic vibrations in amorphous Si. *Phil. Mag. B* **79,** 1715–1731 (1999).
25. Feldman, J. L., Kluge, M. D., Allen, P. B. & Wooten, F. Thermal conductivity and localization in glasses: numerical study of a model of amorphous silicon. *Phys. Rev. B* **48,** 12589–12602 (1993).
26. Regner, K. T. *et al.* Broadband phonon mean free path contributions to thermal conductivity measured using frequency domain thermoreflectance. *Nature Commun.* **4,** 1640 (2013).
27. Osinin, S. & Nosov, M. Relation between the speed of sound and the orientation of chain molecules in anisotropic systems. *Mech. Compos. Mater.* **2,** 4–6 (1966).
28. Cola, B. A. *et al.* Photoacoustic characterization of carbon nanotube array thermal interfaces. *J. Appl. Phys.* **101,** 054313 (2007).
29. Mohammad, F., Calvert, P. D. & Billingham, N. C. Thermal stability of electrochemically prepared polythiophene and polypyrrole. *Bull. Mater. Sci.* **18,** 255–261 (1995).
30. Otiaba, K. *et al.* Thermal interface materials for automotive electronic control unit: trends, technology and R&D challenges. *Microelectron. Reliab.* **51,** 2031–2043 (2011).
31. Cahill, D. G. & Pohl, R. O. Heat flow and lattice vibrations in glasses. *Solid State Commun.* **70,** 927–930 (1989).
32. Choy, C. L., Tong, K. W., Wong, H. K. & Leung, W. P. Thermal conductivity of amorphous alloys above room temperature. *J. Appl. Phys.* **70,** 4919–4925 (1991).
33. Taphouse, J. H. *et al.* Carbon nanotube thermal interfaces enhanced with sprayed on nanoscale polymer coatings. *Nanotechnology* **24,** 105401 (2013).
34. Taphouse, J. H., Smith, O. N. L., Marder, S. R. & Cola, B. A. A pyrenylpropyl phosphonic acid surface modifier for mitigating the thermal resistance of carbon nanotube contacts. *Adv. Funct. Mater.* **24,** 465–471 (2014).

Acknowledgements

This work was supported by the National Science Foundation (NSF; grant no. CBET-1133071), a seed grant from the Georgia Tech Center for Organic Photonics and Electronics and an NSF-IGERT graduate fellowship for T.L.B. The work of Y.C. was supported by the Air Force Office of Scientific Research (award no. FA9550-09-1-0162). The work of K.H.S. was supported by the US Department of Energy, Office of Basic Energy Sciences (award no. DE-SC0002245). The work at UT Austin was supported by the NSF (award no. CBET-0933454). A.W. acknowledges support from the NSF Graduate Research Fellowship Program. K.D.B. was supported by the Natural Science Foundation of China (award no. 51205061), the Natural Science Foundation of Jiangsu Province (award no. BK2012340) and the National Basic Research Program of China (award no. 2011CB707605).

Author contributions

V.S., T.L.B. and B.A.C. conceived and designed the experiments. V.S. prepared the samples and performed the material spectroscopy and adhesion tests. T.L.B. performed the photoacoustic measurements. A.W., K.B., M.T.P., S.A.M. and L.S. performed the microbridge measurements. D.P.R., T.R.G. and D.H.A. performed the SiC chip tests. Y.C. and K.H.S. provided the TEM images and crystallinity characterization. W.L. and A.H. provided the single chain simulations. V.S., T.L.B. and B.A.C. analysed and discussed the data. V.S., T.L.B. and B.A.C. co-wrote the manuscript. All authors commented on the manuscript.

Additional information

Supplementary information is available in the online version of the paper. Reprints and permissions information is available online at www.nature.com/reprints. Correspondence and requests for materials should be addressed to B.A.C.

Competing financial interests

Georgia Tech has applied for a patent, application no. PCT/US 61/484,937, related to the design methods and materials produced in this work. Nanostructured composite polymer thermal/electrical interface material and method for making the same, B.A. Cola, K. Kalaitzidou, H.T. Santoso, V. Singh, US 2012/0285673 A1, November 15, 2012.

CORRIGENDUM

High thermal conductivity of chain-oriented amorphous polythiophene

Virendra Singh, Thomas L. Bougher, Annie Weathers, Ye Cai, Kedong Bi, Michael T. Pettes, Sally A. McMenamin, Wei Lv, Daniel P. Resler, Todd R. Gattuso, David H. Altman, Kenneth H. Sandhage, Li Shi, Asegun Henry and Baratunde A. Cola

Nature Nanotechnology **9,** 384–390 (2014); published online 30 March 2014; corrected after print 17 June 2014.

In the version of this Article originally published, in the section 'Thermal conductivity of individual fibres', the second sentence should have read "The measured thermal conductivity of the several nanofibre samples increases with decreasing diameter…" This error has now been corrected in the online versions of the Article.